Molecular displacements in the spin-dimerized state of (tetrathiafulvalene)$CuS_4C_4(CF_3)_4$ at 4.2 K

J. S. Kasper
General Electric Corporate Research and Development, Schenectady, New York 12301

D. E. Moncton
Bell Laboratories, Murray Hill, New Jersey 07974
(Received 8 May 1979)

We have carried out a crystallographic study of the dimerized state of the spin-Peierls compound (TTF)Cu(BDT). X-ray data taken below the dimerization transition at $T_c = 12$ K were analyzed using a model which assumes rigid molecular displacements. We find that pairing is accomplished by a simple longitudinal translation of spin-$\frac{1}{2}$ $(TTF)^+$ units along the $\vec{c}_p$ axis in the primitive triclinic cell. We use our quantitative measurement of the displacement magnitude ($\Delta x = 0.072$ Å) within the mean-field spin-Peierls model to show that the unrenormalized energy of the dimerization phonon is about 1 meV. This result is consistent with previous observations of preexisting soft modes in x-ray diffuse-scattering studies. Implications for the observation of this transition in other materials are discussed.

I. INTRODUCTION

The instability of a spin-$\frac{1}{2}$ one-dimensional Heisenberg antiferromagnet against spin-lattice dimerization has been expected theoretically[1] and observed experimentally by Jacobs *et al.*[2] in the quasi-one-dimensional charge-transfer salt (TTF)Cu(BDT) (TTF is tetrathiafulvalene, BDT is *bis*-dithiolene). Following these studies specific structural questions were examined by x-ray diffuse scattering.[3] These experiments gave the first direct evidence for dimerization below $T_0 = 12$ K, confirmed the mean-field nature of the transition, and demonstrated that a soft phonon mode exists in the undimerized state which minimizes the elastic energy of dimerization. In addition these studies concluded that one of two unexpected directions must be the one-dimensional chain axis. However, this initial diffraction study stopped short of attempting to determine the low-temperature structure. In the present work we have endeavored to fill that void by providing detailed structural parameters for the dimerized state. These data enable us to resolve the ambiguity of the chain-axis directions and to provide further structural support for the simple picture of pairing between $(TTF)^+$ units. Furthermore, within the spin-Peierls model, determination of displacement magnitudes enables the quantitative calculation of the spatial gradients of the magnetic exchange interaction from which the spin-lattice coupling derives. This calculation then provides a quantitative estimate of the restoring force associated with pairing. We find this force, when expressed as a phonon frequency, to be $\hbar\omega_0 \sim 1$ meV. This low frequency is further evidence of the incipient lattice instability which gives rise to the peak in thermal diffuse scattering observed in Ref. 3. This observation has important implications for the physics of the dimerization transition and these will be discussed.

II. SCOPE OF THE INVESTIGATION

The present experiment was undertaken with a two-circle $(2\theta, \omega)$ instrument incorporating a helium-flow cryostat and a high-intensity 50-kW rotating-anode x-ray source. Intensities as small as 10^{-6} times the strongest main lattice reflection could be accurately measured. One zone of reflections could be studied in a single run with some restrictions imposed by cryostat window design. With two different orientations of crystals we have obtained two zones of accurately determined integrated intensities.

One expects that rigid molecular displacements rather than intramolecular changes are principally responsible for the change of structure below the 12-K transition. Accordingly we assume rigid configurations for the two molecules in our analysis. In this case, twelve parameters suffice to describe the motions of the two molecules and these are determined from the available data set. Although it was our original intent to obtain complete intensity data, we now believe that such an extended study would be severely restricted by radiation damage effects that significantly diminish with time the intensities of superlattice peaks.

 ©1979 The American Physical Society

TABLE I. Lattice constants of (TTF) $CuS_4C_4(CF_3)_4$ at 20 and 4.2 K.

Space group	20 K[a] $P\bar{1}$	4.2 K $B\bar{1}$	4.2 K $P\bar{1}$
a (Å)	8.51	$16.96 = 2 \times 8.48$	11.39
b (Å)	11.43	11.39	13.24
c (Å)	6.76	$13.44 = 2 \times 6.72$	7.68
α	83.4°	83.3°	105.3°
β	120.6°	120.6°	96.8°
γ	101.8°	101.5°	79.3°
V (Å^3)	554.0	4×547.4	547.4

[a]From Ref. 4.

III. EXPERIMENTAL PROCEDURE

Cu $K\alpha$ x rays ($\lambda = 1.5418$ Å) from a 50-kW rotating-anode x-ray tube were focused on the sample using a vertically bent pyrolytic graphite monochromator. A flat crystal of pyrolytic graphite was used as an analyzer after the sample to decrease the background due to extraneous scattering. Integrated intensities were determined from θ-2θ scans. The crystal temperature was always in the range 4.2 to 5 K.

Two crystals, designated as A and B hereafter, were studied. Crystal A was ascertained to be free of twinning and any detectable crystal defects and was used for obtaining intensities of $(h0l)$ (primitive) reflections. Crystal B however was found to be twinned. It provided (hkh) (primitive) intensity data after corrections for the twinning. Both crystals were quite small (volume < 1 mm^3, largest dimension < 0.5 mm) and were completely bathed by the x-ray beam.

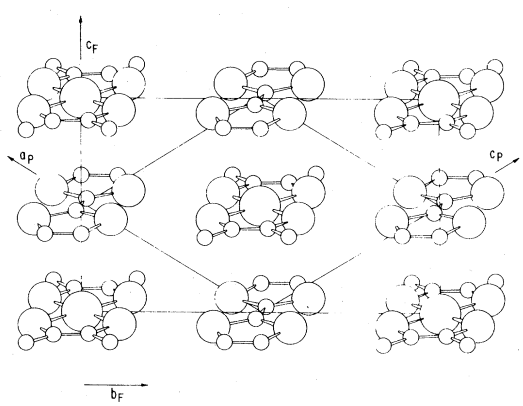

FIG. 1. Arrangement of TTF and Cu(BDT) units in the (010) plane of the primitive triclinic cell. The largest circle represents Cu at the center of a Cu(BDT) unit. The F atoms of BDT and the H atoms of TTF are not shown.

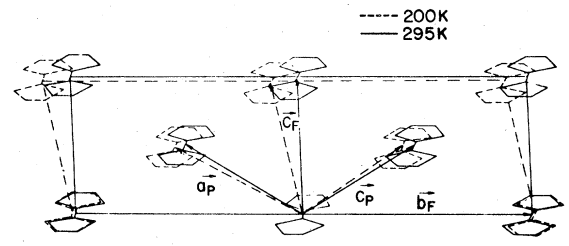

FIG. 2. Illustration of the first-order structural change occurring in the (TTF)$CuS_4C_4(CF_3)_4$ system at 240 K. The $CuS_4C_4(CF_3)_4$ units have been omitted for clarity.

IV. UNIT CELL AND SPACE GROUP

At temperatures above 12 K the unit cell of (TTF)$CuS_4C_4(CF_3)_4$ is triclinic and the space group is $P\bar{1}$. Lattice parameters over a range of temperatures from 20 to 297 K have been determined by Delker.[4] We have relied on Delker's data at 20 K (Table I, column 1) for crystal orientation and indexing in our measurements in the range of 4.2 to 20 K.

The (010) plane of the primitive cell given by Delker is shown in Fig. 1 for the structure at 297 K with the axes a_p and c_p indicated. This plane is also the (100) plane of the face-centered cell which has been sometimes used to describe the structure with axes b_F and c_F as shown. Our discussion will be primarily in terms of the primitive cell.

There is an abrupt structural distortion at ~240 K reflected mainly in changes within the (010) primitive plane as shown in Fig. 2. Notably, the essential equality of a_p and c_p at 297 K is destroyed and c_p becomes 1.8 Å shorter than a_p.

Below 12 K, the new reflections occur with h and l both half-integer values with respect to the primitive cell. Accordingly, both a_p and c_p need to be doubled and the resulting cell is B centered with the parameters of column 2 in Table I. The true cell is primitive, of course, and corresponds to the parameters of column 3 in Table I. The transformation equations are

$$\vec{a}_p' = -\vec{b}_B, \quad \vec{b}_p' = \frac{\vec{a}_B - \vec{c}_B}{2}, \quad \vec{c}_p' = \frac{-\vec{a}_B - \vec{c}_B}{2} .$$

We have used the larger B-centered cell in our structure investigation for the description and discussion of our results, mainly to retain close association to the primitive structure above 12 K.

V. STRUCTURE SOLUTION

The two molecules were considered to be rigid with the configurations determined at 200 K by Delker. The effect of molecular rotations and translations was then investigated using a modified version of the program NUCLS,[5] provided kindly by J. A. Ibers. At most

TABLE II. Observed and calculated structure factors (Crystal *A*).

hkl	F_{obs}	F_{calc}	*hkl*	F_{obs}	F_{calc}
101	0.4	0.2	200	45	50
301	1.5	1.7	400	78	70
501	1.3	2.5	600	19	25
701	1.8	2.1	800	144	145
901	4.6	5.6	10 0 0	14	28
11 0 1	8.2	9.5	12 0 0	51	63
13 0 1	6.2	6.8	002	44	45
103	1.9	1.9	202	24	29
303	2.2	2.2	402	47	47
503	7.5	7.0	602	92	93
703	0.9	0.5	802	35	30
903	7.2	7.4	10 0 2	131	148
11 0 3	5.4	4.6	12 0 2	71	78
13 0 3	2.6	3.9	004	36	41
105	2.4	2.7	204	20	8
305	1.8	1.9	404	105	102
505	4.5	5.2	604	14	9
705	5.5	5.9	10 0 4	26	34
905	2.5	3.6	12 0 4	23	25
11 0 5	3.3	2.7	006	79	77
107	10.8	9.5	206	97	97
307	2.9	1.9	406	107	102
507	1.1	2.3	606	65	41
707	2.3	2.9	806	31	27
907	2.9	3.4	10 0 6	42	41
109	6.8	7.1	008	154	150
309	18.2	17.0	208	7	3
509	7.1	4.4	408	129	120
709	1.8	1.5	608	21	20
$\bar{3}01$	1.0	1.5	$\bar{2}06$	77	66
$\bar{5}01$	2.0	1.9	$\bar{8}06$	45	50
$\bar{7}01$	2.6	1.0	$\overline{10}\ 0\ 6$	72	77
$\bar{9}01$	6.8	7.1	$\bar{8}08$	120	116
$\overline{11}\ 0\ 1$	1.3	2.2	$\overline{10}\ 0\ 8$	31	28
$\bar{1}03$	0.7	0.6	$\overline{12}\ 0\ 8$	36	29
$\bar{1}05$	1.5	1.1	$\overline{14}\ 0\ 8$	59	52
$\bar{1}07$	1.9	0.5	$\overline{16}\ 0\ 8$	83	80
$\bar{3}07$	1.6	1.3	$\overline{10}\ 0\ 10$	71	72
$\bar{7}07$	2.6	1.2	$\overline{12}\ 0\ 10$	14	13
$\bar{9}07$	5.9	5.6	$\overline{14}\ 0\ 10$	36	45
$\overline{11}\ 0\ 7$	4.2	4.5			
$\overline{13}\ 0\ 7$	3.2	3.1		$R = 0.094$	
$\overline{15}\ 0\ 7$	4.3	4.9			
$\overline{17}\ 0\ 7$	4.3	4.3			
$\bar{1}09$	10.5	10.6			
$\bar{9}09$	5.7	6.6			
$\overline{11}\ 0\ 9$	6.1	6.6			
$\overline{13}\ 0\ 9$	0.4	0.7			
$\overline{15}\ 0\ 9$	6.2	5.4			
$\bar{9}\ 0\ 11$	6.6	5.7			
$\overline{11}\ 0\ 11$	2.2	0.8			
$\overline{13}\ 0\ 11$	6.4	4.4			
$\overline{15}\ 0\ 11$	1.6	2.5			
$\bar{9}\ 0\ 13$	2.6	3.4			
$\overline{11}\ 0\ 13$	5.0	3.5			
$\overline{13}\ 0\ 13$	7.6	8.9			
	$R = 0.176$				

TABLE III. Observed and calculated structure factors (Crystal B).

hkl	F_{obs}	F_{calc}	hkl	F_{obs}	F_{calc}
202	24	27	$1\bar{1}1$	1.8	1.0
404	105	102	$1\bar{5}1$	1.2	1.2
$6\bar{3}6$	95	86	$1\bar{6}1$	2.3	2.3
$6\bar{4}6$	201	154	$1\bar{7}1$	4.1	3.5
$4\bar{2}4$	214	181	$1\bar{8}1$	0.0	0.4
$4\bar{3}4$	234	226	$1\bar{9}1$	6.0	6.1
$4\bar{4}4$	41	48	$3\bar{2}3$	0.6	0.5
$4\bar{9}4$	16	9	$3\bar{3}3$	1.2	0.6
$4\ \bar{1}0\ 4$	85	87	$3\bar{4}3$	0.0	0.6
$2\bar{1}2$	359	393	$3\bar{8}3$	2.1	2.5
$2\bar{2}2$	249	265	$3\bar{9}3$	1.2	1.1
$2\bar{3}2$	7	6	$3\ \bar{1}0\ 3$	2.8	3.4
$2\bar{7}2$	41	45	$5\bar{3}5$	1.2	1.7
$2\bar{8}2$	57	51	$5\bar{4}5$	1.6	3.0
$2\bar{9}2$	118	101	$5\bar{9}5$	5.4	5.9
080	130	125	$5\ \bar{1}0\ 5$	0.5	1.0
090	119	118	111	0.2	0.7
0 10 0	96	80	121	0.9	1.0
212	71	54	131	1.4	1.6
222	77	50	$3\bar{1}3$	1.2	0.9
232	150	125	313	2.7	3.5
$4\bar{1}4$	11	10	323	3.3	3.5
414	0	0	333	1.6	1.6
424	92	104	343	0.5	0.6
434	31	32	353	1.5	0.8
444	135	155	$5\bar{2}5$	1.0	1.6
454	117	136	515	4.2	3.4
			525	0.7	1.9
	$R=0.118$		535	1.2	1.1
			545	3.3	4.3
			555	0.0	0.5
			565	1.7	2.5
			$7\bar{2}7$	4.8	3.7
			$7\bar{1}7$	8.3	6.7
			717	3.8	4.0
			727	4.3	3.6
			737	1.5	1.5
			747	5.0	4.1
				$R=0.214$	

twelve parameters, six for each molecule, were required to characterize the molecular displacements.

As a check on the suitability of the 200 K parameters, some integrated intensities were measured at 20 K for $(h0l)$ reflections with h and l even ($B\bar{1}$ cell). These intensities, incidentally, were not significantly different from those measured at 4 K. Their agreement with the values calculated with the 200 K parameters was only moderate ($R=0.20-0.25$) indicating a need for better parameters for 20 K and lower temperatures. It was found that considerable improvement could be made by allowing small adjustments (less than 2°) in the rotational parameters of the molecules. The R value decreased then to 0.095 as shown in Table II for reflections with h and l both even. Maintaining the rotational parameters but allowing the translational parameters to vary it was then possible to achieve satisfactory intensity agreement for the superlattice reflections (h and l both odd) for small displacements of the molecules. Eventually, both rotational and translational parameters were varied, but the former were not altered significantly from the values obtained by considering the nonsuperlattice reflections only. The structure factors are given in Table II.

No evaluation of temperature factors could be

TABLE IV. TTF ($S_4C_6H_4$). Translations $\Delta x = 0.0006(1)$, $\Delta y = 0.0001(2)$, $\Delta z = 0.0027(1)$. Atomic parameters.

	10^4x	10^4y	10^4z
C(5)	2697	582	5225
S(3)	2468	1206	6126
S(4)	3483	1463	4908
C(6)	3172	2541	6203
C(7)	3647	2665	5684
C(5)′	2314	−583	4829
S(3)′	2544	−1207	3929
S(4)′	1529	−1464	5147
C(6)′	1839	−2542	3852
C(7)′	1365	−2665	4370
H(1)′	893	−3341	4344
H(2)′	1773	−3001	3426
H(1)	4119	3337	5710
H(2)	3239	2997	6628

TABLE V. Cu(BDT) ($CuS_4C_8F_{12}$). Translations $\Delta x = 0.0010(2)$, $\Delta y = -0.0008(20)$, $\Delta z = 0.0010(2)$. Atomic parameters.

	10^4x	10^4y	10^4z
Cu	10	−8	2510
S(1)	−965	−1405	2730
S(2)	73	−1118	1359
C(1)	−1018	−2614	2010
C(2)	−537	−2490	1433
S(1)′	982	1387	2287
S(2)′	−53	1102	3661
C(1)′	1038	2598	3010
C(2)′	557	2474	3587
C(3)	−1622	−3733	2076
F(1)	−1123	−4446	2885
F(2)	−2231	−3508	2355
F(3)	−2108	−4372	1132
C(3)′	1642	3716	2944
F(1)′	1143	4429	2135
F(2)′	2251	3491	2665
F(3)′	2128	4355	3888
C(4)	−519	−3482	803
F(4)	−490	−4514	1330
F(5)	218	−3277	682
F(6)	−1248	−3666	−215
C(4)′	539	3465	4217
F(4)′	510	4498	3690
F(5)′	−198	3260	4338
F(6)′	1268	3649	5236

made. They were tested by trial and error and the following isotropic values were used:

$$B_{Cu} = 0.1\ (\text{Å}^2),\quad B_S = 0.2\ (\text{Å}^2)\ ,$$

$$B_C = 0.4\ (\text{Å}^2),\quad B_F = 0.4\ (\text{Å}^2)\ ,$$

$$B_H = 0.4\ (\text{Å}^2)\ .$$

An important complication regarding the superlattice intensities was their significant decrease with time while irradiated by x rays. It was necessary to evaluate the time constant for this process and then obtain integrated intensities with a record of the time of the measurement. The intensity decrease followed an exponential function $I/I_0 = e^{-t/T}$, $1/T = 0.0213\ \text{hr}^{-1}$. Superlattice intensities were corrected accordingly. No significant change in the main reflections (h and l both even) was detected.

Measurements of hkh intensities also were made to verify the previous findings and to ascertain any displacements out of the a-c plane. Unfortunately, the crystal (B) turned out to be twinned. Allowance for the twinning could be made, however, to give only somewhat less satisfactory intensity agreement than the $h0l$ data. The hkh structure factors are given in Table III. The calculated values are for the same x and z displacements obtained with $h0l$ data but with y displacements allowed. Essentially no displacement from the a-b plane was indicated—for TTF $\Delta y = 0.0001(2)$ and for BDT $\Delta y = 0.0008(20)$.

The coordinates for TTF are given in Table IV and those for BDT in Table V. The numbering system is indicated in Fig. 3 and the corresponding interatomic distances are listed in Table VI. Also given in Tables IV and V are the displacements Δx, Δy, Δz of the centers of the molecules from the positions where there is no superlattice and the structure is essentially that above 12 K. The origin of the cell is midway between molecules and displaced by $\frac{1}{4}$ in z from the origin for the cell above 12 K which contains the Cu atom of BDT.

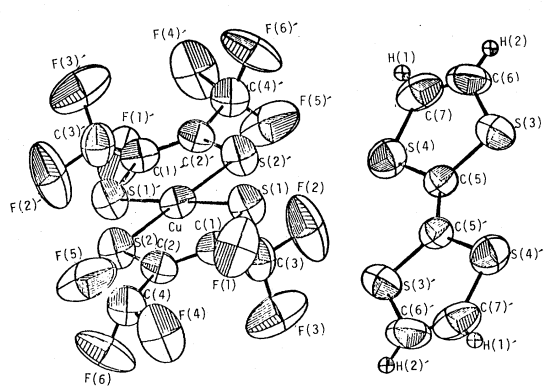

FIG. 3. Numbering system used for $(TTF)CuS_4S_4(CF_3)_4$.

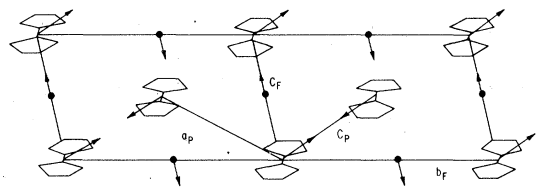

FIG. 4. Directions of displacements for the $(TTF)^+$ and $CuS_4(CF_3)_4^-$ units (only the center of mass of the latter species is shown here, for clarity) below the spin-Peierls transition temperature.

The most significant result is the displacement of the TTF molecule along z by 0.0027(1) or 0.036 Å. It appears that there is also a smaller displacement of 0.015Å of the BDT molecules along the short diagonal direction. A schematic illustration of the displacements is given in Fig. 4.

VI. DISCUSSION

Although our data were limited by the combined difficulties of obtaining helium temperatures and measuring very low-peak intensities, we have succeeded in answering all the physically relevant structural questions pertaining to this unusual phase transition. We have removed the ambiguity concerning the dimerization axis and established the primitive $\vec{c}$ direction as the one-dimensional (1-D) chain axis. We have shown that the predominant molecular motion is associated with the spin-$\frac{1}{2}$ $(TTF)^+$ molecule, as expected in the spin-Peierls model, accompanied by a smaller secondary motion of the BDT molecules. Furthermore, the $(TTF)^+$ motion is a simple pairing, which not only provides additional support for the spin-dimerization picture, but indicates that direct exchange is the dominant magnetic interaction.

In addition to these qualitative observations, our quantitative determination of the pairing displacements of $(TTF)^+$ molecules allows the use of the spin-Peierls model to determine the elastic energy cost associated with the $(TTF)^+$ motion. It is thus possible to shed further light on the role of the preexisting soft phonon observed in the previous x-ray study.[3]

From the mean-field theory of Pytte[1] we start with the expression for the transition temperature[6]

$$T_c = 0.83pJe^{-1/\lambda p} \quad , \tag{1}$$

where p is a slowly varying function of temperature [we take $p(T) = p(0) = 1.637$ after Ref. 2] and $J = 77$ K is the exchange interaction. Here λ is the coupling parameter given by

$$\lambda = \frac{4(\nabla J)^2}{C\pi J} \quad , \tag{2}$$

TABLE VI. Interatomic distances (Å) for (TTF) $CuS_4C_4(CF_3)_4$ at 4.2 K.

$CuS_4C_4(CF_3)_4$		TTF	
Cu-S(1)	2.171	C(5)-C(5)	1.392
Cu-S(2)	2.173	C(5)-S(3)	1.715
S(1)-C(1)	1.739	C(5)-S(4)	1.709
S(2)-C(2)	1.718	S(3)-C(6)	1.714
C(1)-C(2)	1.368	S(4)-C(7)	1.716
C(1)-C(3)	1.493	C(6)-C(7)	1.292
C(2)-C(4)	1.507	C(6)-H(2)	0.90
C(3)-F(1)	1.311	C(7)-H(1)	0.90
C(3)-F(2)	1.339		
C(3)-F(3)	1.319		
C(4)-F(4)	1.303		
C(4)-F(5)	1.317		
C(4)-F(6)	1.306		

where $C = M\omega_0^2$ is the unrenormalized elastic constant for the dimerization phonon. To obtain ∇J we note the relation

$$\nabla J = J\frac{\delta}{\Delta x} \quad , \tag{3}$$

where δ is defined for the dimerized chain by

$$J_{1,2} = J(1 \pm \delta) \tag{4}$$

and $\Delta x = 0.072$ Å as determined by our structural study. From fits to the magnetization data Jacobs *et al.*[2] obtained $\delta(0) = 0.127$. Using the above equations we find $C = 9.1 \times 10^{14}$ eV/cm^2. The phonon associated with dimerization then has an energy $\hbar\omega_0 = \hbar(C/m)^{1/2}$. Using the mass for a TTF unit alone, since the BDT motion is small, we find that $\hbar\omega_0 = 1.4$ meV. Although this energy is unusually small for a zone-boundary phonon, it is consistent with the soft mode observed in x-ray diffuse scattering.

Recently Cross and Fisher[7] have developed a new theory of the transition based on an improved treatment of the pseudo-fermion spin system. Unlike Pytte, they find the following linear relation between transition temperatures and coupling constant:

$$T_c = 0.8J\lambda \quad . \tag{5}$$

Using a similar analysis, the phonon frequency $\hbar\omega_0 = 1.7$ meV is obtained.

In conclusion, we emphasize the importance of this soft mode. It is obvious that the dimerized state occurs in (TTF)Cu(BDT) at a temperature sufficiently high that the 3-D Néel state which occurs in other 1-D Heisenberg antiferromagnets is preempted. The dependence of the transition temperature on the inverse square of the phonon frequency ω_0 implies that an increase in ω_0 leads to a large reduction in T_c.

Therefore, dimerization in this system is favored over magnetic ordering because the phonon frequency is anomalously low. Further, one expects the transition temperature to be extremely sensitive to structural (as opposed to magnetic) changes which would alter the phonon frequency. Indeed both the isostructural (TTF)Cu(BDSe) {Cu(BDSe) is *bis* [di - 1,2 (trifluoromethyl) ethylene - 1,2 - diselenolate] copper (II)} (Ref. 8) and (TTF)Au(BDT) (Ref. 2) have similar magnetic exchange energies J but much lower transition temperatures (6.0 and 2.0 °K, respectively). Finally, the general lack of other examples of the phase transition can be explained by the absence of a suitable soft phonon. Perhaps it is not surprising that a new spin-Peierls material (MEM)$(TCNQ)_2$ (N-methyl-N-ethyl-morpholinium ditetracyanoquinodimethanide) has recently been discovered,[9] and it too has been shown to exhibit a soft phonon. Of course, it is always possible that a system which has no unusually soft phonon could undergo a dimerization if the exchange gradient is sufficiently large.

ACKNOWLEDGMENTS

We are very grateful to J. W. Bray for his thoughtful consideration of the physical implications of the crystallographic distortion and to L. V. Interrante for providing the crystals used in this investigation. Also one of us (D. E. Moncton) is happy to acknowledge helpful conversations with M. C. Cross and D. S. Fisher.

[1]See, E. Pytte, Phys. Rev. B 10, 4637 (1974); and the historical account given in Ref. 2.

[2]I. S. Jacobs, J. W. Bray, H. R. Hart, Jr., L. V. Interrante, J. S. Kasper, G. D. Watkins, D. E. Prober, and J. C. Bonner, Phys. Rev. B 14, 3036 (1976).

[3]D. E. Moncton, R. J. Birgeneau, L. V. Interrante, and F. Wudl, Phys. Rev. Lett. 39, 507 (1977).

[4]G. L. Delker, Ph.D. thesis (University of Illinois, 1976) (unpublished).

[5]NUCLS5— Program for refinement of rigid groups, J. A. Ibers, Northwestern University.

[6]The prefactor of 0.83 has been calculated by J. W. Bray and agrees with the recent work of M. C. Cross and D. Fisher. Numerical errors existed in previous work (Refs. 1 and 2).

[7]M. C. Cross and D. S. Fisher, Phys. Rev. B 19, 402 (1979).

[8]B. Hoffman, P. Piacente, L. V. Interrante, and H. R. Hart, Jr. (unpublished).

[9]H. A. Mook, B. C. Larson, and B. van Bodegom, Bull. Am. Phys. Soc. 24, 355 (1979).